

Chapter 4

Tkachenko Modes [3]

4.1 Introduction

We have all seen a cylindrically confined fluid support azimuthal flow whether we are watching water flow down a drain or a recently stirred cup of coffee. What is somewhat harder to imagine is a fluid sustaining oscillatory azimuthal flow. Instinctively one does not expect a fluid to support shear forces, and this would seem especially true in the case of zero-viscosity superfluids, but such intuition is incomplete.

The key issue is vortices. In 1955, Feynman [16] predicted that a superfluid can rotate when pierced by an array of quantized singularities or vortices. In 1957, Abrikosov [74] demonstrated that such vortices in a type II superconductor will organize into a triangular crystalline lattice due to their mutual repulsion. Not surprisingly, the Abrikosov lattice has an associated rigidity. In 1966, Tkachenko proposed that a vortex lattice in a superfluid would support transverse elastic modes [26]. First observed by Andereck *et al.*[27], Tkachenko oscillations have been the object of considerable experimental and theoretical effort in superfluid helium, much of which was summarized by Sonin in 1987 [75].

In the last two years it has become possible to achieve a vortex lattice state in dilute gas BEC [22, 24, 23, 25] and recent theoretical work [28] has suggested that Tkachenko oscillations are also attainable. In this chapter I discuss the observation of Tkachenko oscillations in BEC. The particular strengths of BEC are that in the clean en-

environment of a magnetically trapped gas there is no vortex pinning, and spatiotemporal evolution of the oscillation may be directly observed.

When we started our experimental investigation of Tkachenko modes, the only theory available to compare to was the one given in [28] by Anglin and Crescimanno. As described during the discussion of our experimental work in the following section, the oscillation frequencies predicted by this initial theory were not in excellent quantitative agreement with our experiments. As I will describe in §4.6, it was later pointed out by Gordon Baym that a more adequate theory for our experiments needs to account for compressibility effects of the lattice. This hints at a major difference between Tkachenko wave experiments in liquid Helium and in dilute gas BECs: Our experiments reach into a new regime that lies outside the region accessible with liquid Helium experiments.

4.2 Exciting Tkachenko modes

As before we begin this experiment with a rotating condensate held in an axially symmetric trap with trap frequencies $\{\omega_\rho, \omega_z\} = 2\pi\{8.3, 5.2\}$ Hz. The condensed cloud contains 1.5-2.9 million ^{87}Rb atoms in the $|F = 1, m_F = -1\rangle$ state. The cloud rotates about the vertical, z axis. Condensate rotation rates (Ω) for the experiments described in this chapter range from $\Omega = 0.84\omega_\rho$ to $\Omega = 0.975\omega_\rho$ (Ω defined as condensate rotation rate divided by ω_ρ). We have no observable normal cloud implying a $T/T_c < 0.6$. As before, rotation can be accurately measured by comparing the condensate aspect ratio to the trap aspect ratio using equation 2.2. Vortices, which are too small to observe in trap, can be seen by expanding the cloud as detailed in §2.3. At our high rotation rates the condensate is oblate and the vortex cores are essentially vertical lines except right at the surface.

We excite lattice oscillations by two mechanisms. The first mechanism presented is based on the selective removal of atoms that has also been discussed in §3.2. With this method we remove atoms at the center of the condensate with a resonant, focused laser

beam sent through the condensate along the axis of rotation. The width of the “blasting” laser beam is $16 \mu\text{m}$ FWHM (small compared to an in-trap condensate FWHM of $75 \mu\text{m}$), with a Gaussian intensity profile. The frequency of the laser is tuned to the $F'' = 1 \rightarrow F' = 0$ transition of the D2 line, and the recoil from a spontaneously scattered photon blasts atoms out of the condensate. The laser power is about 10 fW and is left on for approximately one lattice rotation period (125 ms).

The effect of this blasting laser is to remove a small (barely observable) fraction of atoms from the center of the condensate. This has two consequences. First, the average angular momentum per particle is increased by the selective removal of low angular momentum atoms from the condensate center. This increase then requires a corresponding increase in the equilibrium condensate radius [76]. Secondly, the atom removal creates a density dip in the center of the cloud. Thus, after the blasting pulse, the condensate has fluid flowing inward to fill the density dip and fluid flowing outward to expand the radius. The Coriolis force acting on these flows causes the inward motion to be diverted in the lattice rotation direction and the outward flow to be diverted in the opposite direction. This sheared fluid flow drags the vortices from their equilibrium configuration and sets the initial conditions for the lattice oscillation as can be seen from the expanded images in figure 4.1.

The second method of exciting the Tkachenko oscillation is essentially the inverse of the previous method. Instead of removing atoms from the cloud we use a red-detuned optical dipole potential to draw atoms into the middle of the condensate. To do this we focus a 850 nm laser beam onto the condensate. The beam has $3 \mu\text{W}$ of power and a $40 \mu\text{m}$ FWHM. It propagates along the direction of condensate rotation and its effect is to create a 0.4 nK deep Gaussian dip in the radial trapping potential. This beam is left on for 125 ms to create an inward fluid flow similar to before. The resulting Tkachenko oscillation was studied for $\Omega = 0.95\omega_\rho$, and found to be completely consistent with the atom removal method. It is not surprising that these two methods are equivalent since

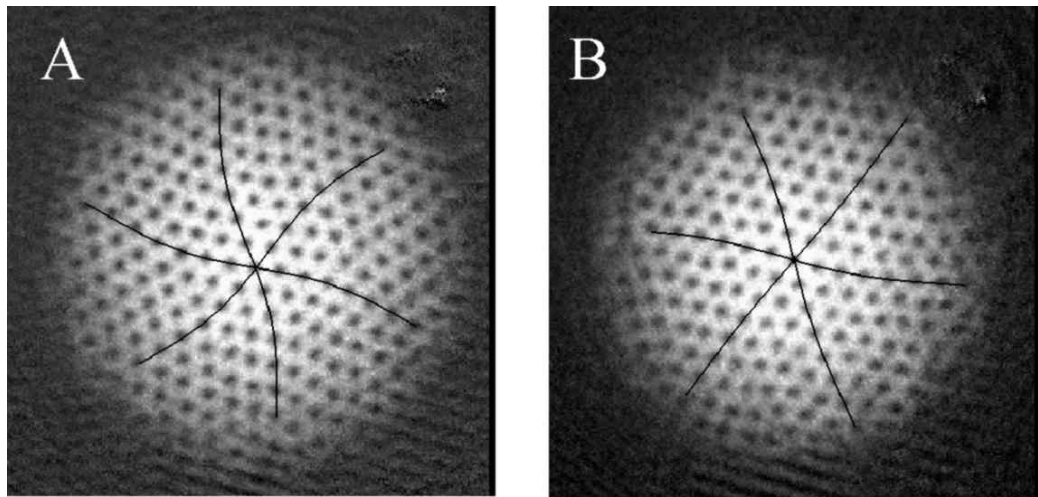


Figure 4.1: $(1,0)$ Tkachenko mode excited by atom removal (a) taken 500 ms after the end of the blasting pulse (b) taken 1650 ms after the end of the blasting pulse. BEC rotation is counterclockwise. Lines are sine fits to the vortex lattice planes.

one works by creating a dip in the interaction potential and the other creates a similar dip in the trapping potential.

For these experiments, data is extracted by destructively imaging the vortex lattice in expansion and fitting the lattice oscillation. To perform this fit we find a curvilinear row of vortices going through the center of the cloud and fit a sinewave to the locations of the vortex centers, recording the sine amplitude. This is done for all three directions of lattice symmetry [see figure 4.1], with the amplitudes averaged to yield the net fit amplitude of the distortion.

4.3 The (1,0) mode

The resulting oscillation [see figure. 4.2] is heavily damped and has a Q value of 3-5 for the data presented. Here Q is given by $Q=2\pi f\tau_{damping}$, where $\tau_{damping}$ is the exponential-damping time constant for the oscillation. We are able to increase this to a Q of 10 by exciting lower amplitude oscillations (40% of the previous amplitude) and by better mode matching of the blasting beam to the shape and period of the oscillation (40 μm FWHM beam width and 500 ms blasting time). Measured frequencies for the high-amplitude oscillations are the same as for the low-amplitude, high-Q case so we do not believe that we are seeing anharmonic shifts¹.

Because of the characteristic s-bend shape and the low resonant frequency of these oscillations [see figure 4.3(a)] we interpret them to be the (n=1,m=0) Tkachenko oscillations predicted by Anglin and Crescimanno [28]. Here (n,m) refer to the radial and angular nodes, respectively, in the presumed quasi-2-D geometry. The calculations of Ref.[28] predict that these lattice oscillations should have a frequency of $\nu_{10} = 1.43\epsilon\Omega/(2\pi)$ for the (1,0) mode and $\nu_{20} = 2.32\epsilon\Omega/(2\pi)$ for the (2,0) mode. Here $\epsilon = b/R_\rho$ denotes the nearest-neighbor vortex spacing, b, over the radial Thomas-Fermi radius, R_ρ . For our

¹ Note that for all cases the reported frequency is adjusted for damping according to the equation $f_o = 1/2\pi((2\pi f_{measured})^2 + (1/\tau_{damping})^2)^{1/2}$.

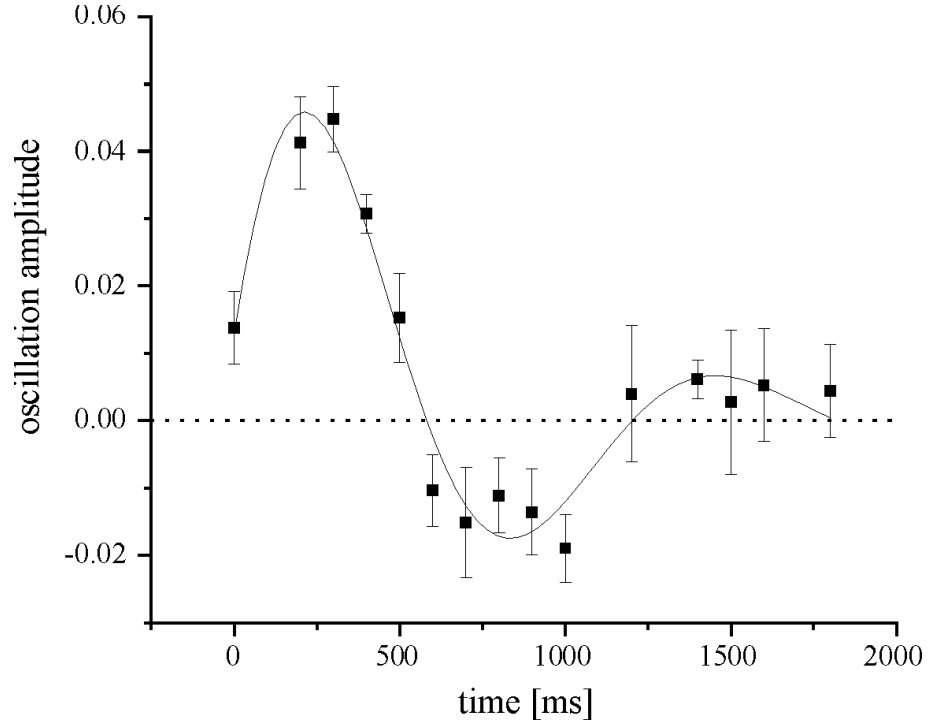


Figure 4.2: Measured oscillation amplitude for a typical excitation. Data shown is for a BEC rotating at $\Omega = 0.92\omega_\rho$ and containing 2.2×10^6 atoms. Fit is to a sinewave times an exponential decay and yields a frequency of 0.85 Hz and a Q of 3. The oscillation amplitude is expressed as the average amplitude of the sinewave fits to the vortex oscillation in units of the radial Thomas-Fermi radius (roughly the azimuthal displacement of a vortex a distance $0.33 R_\rho$ from the condensate center). Both values are in expansion.

system these predicted frequencies are around 1-2 Hz and are therefore far slower than any of the density-changing coherent oscillations of the condensate except for the $m=-2$ surface wave [25, 77, 40, 78]. In addition, the shape of the observed oscillation agrees well with theory. Specifically, the prediction[28] that the spatial period of a sinewave fit to a row of vortices in a (1,0) oscillation should be $1.33 R_\rho$ is in perfect agreement with our data.

The predicted frequencies are, however, problematic. To make the comparison to the theory presented in Ref.[28] we excite lattice oscillations in the condensate for $\epsilon\Omega/\omega_\rho$ ranging from 0.10 to 0.15. This is achieved by varying number and rotation rate. Over this range of $\epsilon\Omega$ the oscillation frequencies measured are consistently lower than those predicted by theory as can be seen in figure 4.3(b). For the slowest rotations, $\Omega = 0.84\omega_\rho$ ($\epsilon\Omega/\omega_\rho = 0.15$, $N=2.5 \times 10^6$), we observe frequencies that are as close as 0.70 of the predicted value. However, at larger rotation rates, $\Omega = 0.975\omega_\rho$ ($\epsilon\Omega/\omega_\rho = 0.10$, $N=1.7 \times 10^6$), the agreement is considerably worse (the measured value is 0.31 of the predicted value). One possible explanation for this general discrepancy is that the calculations are done in 2-D and ignore the issues of vortex bending at the boundary and finite condensate thickness [79]. In those cases, however, one would expect better agreement at high rotation rates where the condensate aspect ratio is more 2-D. A more likely explanation is that the continuum theory, used in the Anglin and Crescimanno calculation, is breaking down as the vortex core size to vortex spacing becomes finite [79]. This suggests that at high rotation and lower atom number we are entering a new regime. To further explore this possibility we reduced the atom number to $N=7-9 \times 10^5$, while keeping $\epsilon\Omega/\omega_\rho$ roughly the same. This should increase the core size and exacerbate the problem. As can be seen in figure 4.3(b) and figure 4.3(c) the agreement with theory is significantly worse under these conditions. These discrepancies will be discussed in more detail in §4.6.

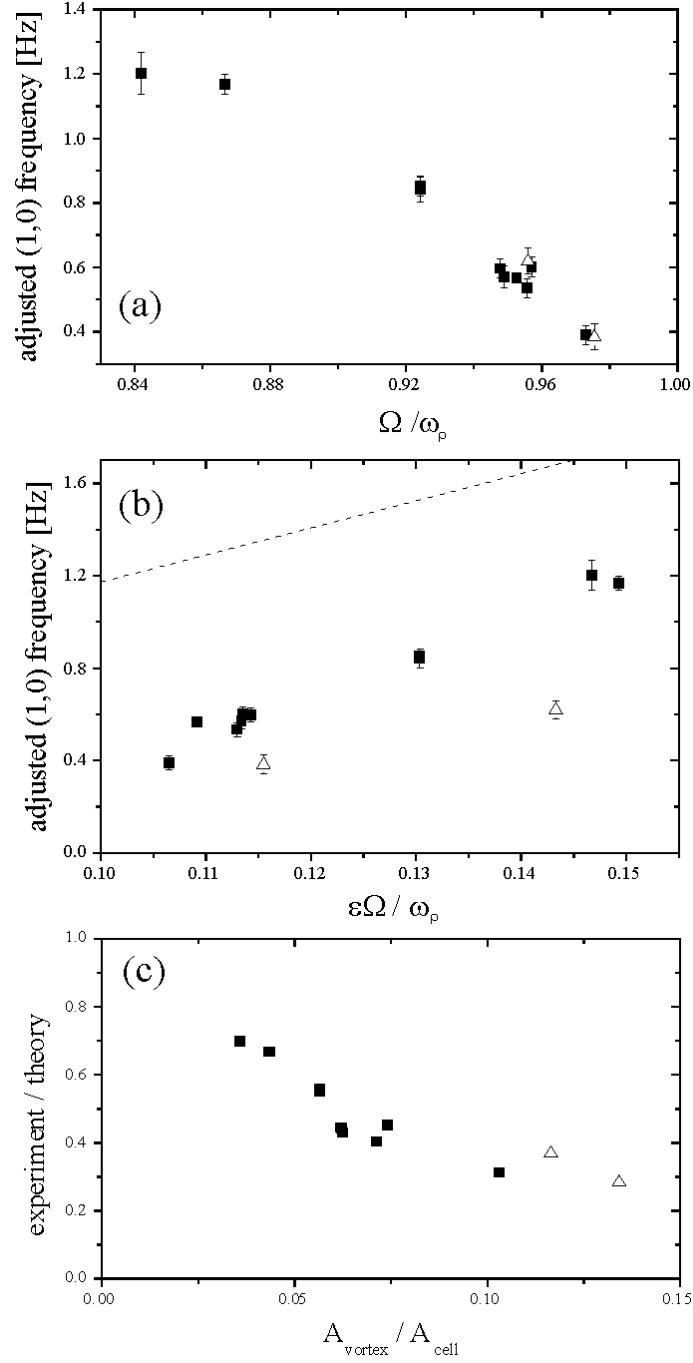


Figure 4.3: Plot (a) shows the damping-adjusted ($n=1, m=0$) Tkachenko oscillation frequencies as a function of scaled rotation rate Ω/ω_p . Plot (b) shows the (1,0) frequency as a function of the theory parameter $\epsilon\Omega/\omega_p$. The dotted line is the theory line $\nu_{10} = 1.43\epsilon\Omega/(2\pi)$ from Ref. [28]. Note that the low number data shows much worse agreement with theory. Plot (c) demonstrates the divergence of experimental frequency from the theory frequency as the ratio of vortex core area to unit cell area increases. A_{vortex} is $\pi\xi^2$ where the healing length $\xi = (8\pi na)^{-1/2}$ (here n is density-weighted average density and a is the s-wave scattering length). Lattice cell area A_{cell} is $\sqrt{3}b^2/2$ (here b is the nearest-neighbor vortex spacing). For all plots black squares and triangles refer to high and low atom number experiments, respectively.

4.4 The (2,0) mode

We are also able to excite the (2,0) mode. We note that atom removal creates an s-bend in the lattice that is centered on the atom removal spot. To write two s-bends onto the lattice one could imagine removing atoms from an annular ring instead of a spot. To make this ring we offset the blasting beam half a condensate radius and leave it on for 375 ms (three full condensate rotation periods). As one can see this does lead to an excitation of the (2,0) oscillation (see figure 4.4). We measure the frequency of this mode as before. For 2.3 million atoms and $\Omega = 0.95\omega_\rho$ we measure a lattice oscillation frequency of 1.1 ± 0.1 Hz, distinctly lower than the theoretical prediction [28] of 2.2 Hz for our parameters.

4.5 Bulk fluid modes

Vortex motion and condensate fluid motion are intimately linked [75]. In Tkachenko oscillations, the moving of vortices must also entail some motion of the underlying fluid, and pressure-velocity waves in the fluid must conversely entrain the vortices. Very generally, for a substance composed of two interpenetrating materials, one of which has an elastic shear modulus and one of which does not (in our case, the vortex lattice and its surrounding superfluid, respectively), one expects to find three distinct families of sound waves in the bulk: (i) a shear, or transverse, wave, (ii) a common-mode pressure or longitudinal wave, and (iii) a differential longitudinal wave, with the lattice and its fluid moving against one another [80]. The presence of strong Coriolis forces makes the distinction between longitudinal and transverse waves problematic, but the general characteristics of the three families should extend into the rotating case. For instance, one can still readily identify the Tkachenko modes discussed thus far as the transverse wave. Our assumption is that the common-mode longitudinal waves are nothing other than the conventional hydrodynamic shape oscillations studied previously [40, 78].

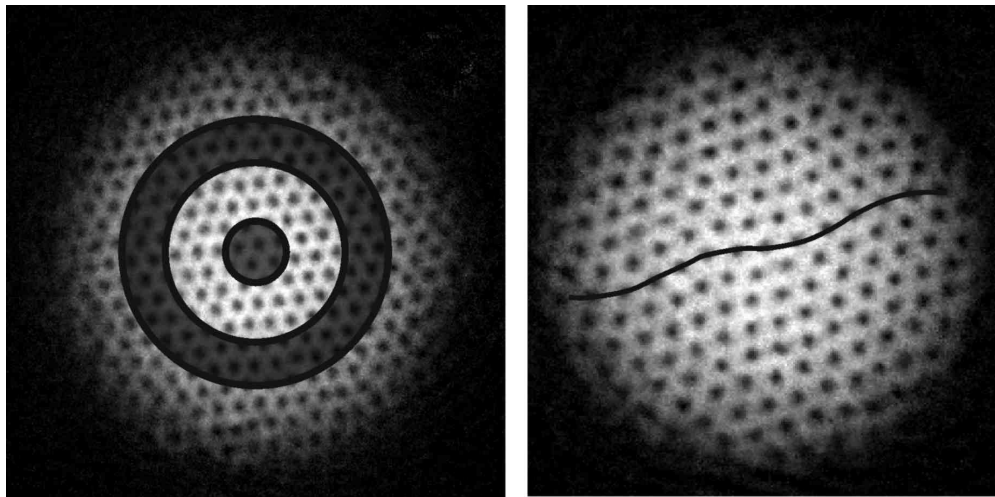


Figure 4.4: On the left are the locations where atoms are removed from the cloud. For the $(1,0)$ excitations the atoms are removed from the shaded region in the center. For the $(2,0)$ mode atoms are removed from the shaded ring half a condensate radius out. Image on the right is the resulting $(2,0)$ mode, where the black line has been added to guide the eye.

To excite the common-mode longitudinal wave, we use the dipole force from the 850 nm red-detuned laser described earlier. In order to excite a broad spectrum of modes we shorten the laser pulse to 5 ms, widen the excitation beam to a 75 μm FWHM Gaussian profile, and increase the laser power to 1 mW, resulting in a 30 nK deep optical potential. We find that this pulse excites three distinct $m=0$ modes: the first is the (1,0) Tkachenko s-bend mode at about 0.6 Hz already discussed. The second is a radial breathing mode in which the condensate radius oscillates at 16.6 ± 0.3 Hz (or $2.0 \pm 0.1 \frac{\omega_\rho}{2\pi}$). This mode has been previously observed [81], and our observed frequency is consistent with hydrodynamic theory for a cloud rotating at $\Omega = 0.95\omega_\rho$ [40]. As the radius of the fluid density oscillates, so does the mean lattice spacing of the vortex lattice, but we observe no s-type bending of the lattice at this frequency. The fact that the frequency of the lowest $m=0$ radial longitudinal mode is more than 20 times that of the transverse mode demonstrates how relatively weak the transverse shear modulus is.

The same laser pulse excites a third mode, at the quite distinct frequency of 18.5 ± 0.3 Hz. This mode manifests as a rapid s-bend distortion of the lattice indistinguishable in shape from the 0.6 Hz (1,0) Tkachenko oscillation as can be seen in figure 4.5. 18.5 Hz is much too fast to have anything to do with the shear modulus of the lattice, and we were very tempted to identify this mode as a member of the third family of sound-waves, the differential longitudinal waves. Simulations by Cozzini and Stringari [82, 83], however, show that our observed frequency is consistent with a higher-order, hydrodynamic mode of the rotating fluid that can be excited by an anharmonic radial potential such as our Gaussian optical potential. Moreover, they show that the radial velocity field of their mode is distorted by Coriolis forces so as to drag the lattice sites into an azimuthally oscillating s-bend distortion that coincidentally resembles the Tkachenko mode. It is worth noting that without the presence of the lattice to serve as tracers for the fluid velocity field, it would be very difficult to observe this higher-order mode, since this mode has very little effect on the mean radius of the fluid. In any case, the mode at

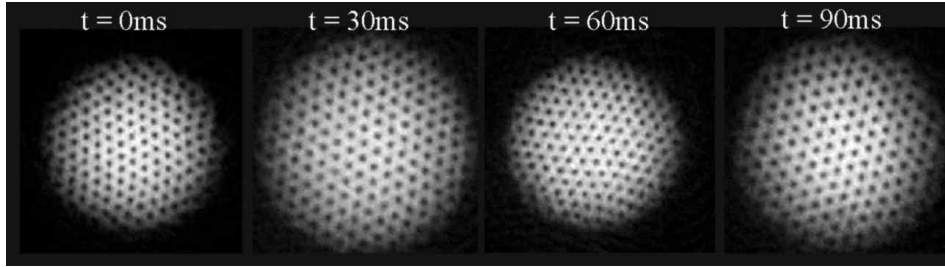


Figure 4.5: Radial breathing mode and fluid flow driven lattice bending as observed after a dipole beam pulse. For parameters, see text.

18.5 Hz appears to be yet another member in the family of common-mode longitudinal waves. The discovery of this longitudinal mode demonstrates the usefulness of vortices to visualize complicated hydrodynamic flow patterns in a BEC. So far we have been unable to observe a mode we can assign to the family of differential longitudinal waves.

4.6 Theory responds

In section §4.2 and in our original Tkachenko [84] paper, I suggest that our discrepancy with the Anglin and Ciccimanno prediction, seen in figure 4.3, is due to the finite size of the vortex cores, which turns out not to be completely true. Finite core size turns out to be tantamount to saying that we are approaching the lowest Landau level (described in more detail in §5). As it happens, the lowest Landau level dynamics describe only a small part of this discrepancy. Since the original publishing of the Tkachenko paper there has been an extensive theory response [29, 83, 31, 85, 33, 86, 32]. A central point of nearly all these works is that lattice compressibility must be taken into account to describe the Tkachenko oscillation in BEC's.

In a highly rotating condensate the rotation rate can easily approach or even exceed the speed of sound in the condensate. As the speed of sound is approached, the lattice becomes compressible, and enters a regime not accessible to superfluid Helium systems. This compressibility also means that higher-order terms must be taken into account when determining the Tkachenko dispersion relation. As noted by Baym [29,

87, 88] the dispersion relation

$$\nu(k)^2 = \frac{1}{(2\pi)^2} \frac{2C_2}{nm} \frac{s^2 k^4}{(4\Omega^2 + (s^2 + 4(C_1 + C_2)/nm)k^2)}. \quad (4.1)$$

Here n is the condensate density² and m is the mass of Rubidium. The wave number k for the (1,0) mode is taken, from Anglin and Crescimanno [28], to be $k_{(1,0)} = 2\pi/(1.33R_\rho)$ and s is the speed of sound. C_1 and C_2 are the compressional and shear modulus of the lattice respectively. In the incompressible limit, one would expect that $C_2 = -C_1 = n\Omega/8$. However, as Baym notes, the shear modulus weakens with higher rotation and as one approaches the lowest Landau level C_2 , is known to have the form $C_2 \simeq (81/80\pi)ms^2n$ [29, 87, 88]. The exact nature of the transition between these two limits has not been rigorously determined.

Equation 4.1 can be broken into two interesting regimes. At low rotations ($\Omega \ll sk$), equation 4.1 simplifies to

$$\nu(k) = \frac{1}{2\pi} \sqrt{\frac{2C_2}{nm}} k. \quad (4.2)$$

This low rotation regime is often referred to as the “stiff” Thomas Fermi regime. In this regime, Tkachenko oscillations are expected to behave much like they do in superfluid helium systems, and the theory presented in Ref. [28] would be more appropriate. However, one notes that in our system $sk_{(1,0)} \simeq 0.66\omega_\rho$, which means that we are well out of this regime by the time our vortex lattices are large enough to observe a Tkachenko oscillation.

Alternatively, at high rotations ($\Omega \gg sk$) one enters the “soft” Thomas-Fermi regime where equation 4.1 simplifies to

$$\nu(k) = \frac{1}{2\pi} \sqrt{\frac{s^2 C_2}{2\Omega^2 nm}} k^2. \quad (4.3)$$

The Tkachenko data presented in this thesis generally lies between these two regimes or in the “soft” regime. This second dispersion relation is striking in its’ quadratic

² Baym uses peak density in his original paper but we have found that density-weighted density provides an equally good fit to the data and requires less fudging with the C_2 parameter. Density-weighted density also would seem appropriate as the Tkachenko excitation exists over the entire cloud.

behavior and is expected to lead to loss of long range phase coherence in the condensate [85]. Ultimately this loss of phase coherence is expected to lead to melting of the vortex lattice as one approaches the quantum Hall regime [89].

The Bigelow group has spent some time using numerics to examine the difference between these two regimes. A striking difference in the flow patterns in these two regimes can be seen in figure 4.6 which was provided by L. O. Baksmaty [83].

Interesting work has also been done on the condensate density profile during a Tkachenko oscillation. Using a sum rule method Cozzini **et al.** [32] has demonstrated that the condensate density profile dips slightly ($\sim 5\%$) in the center and the outer edge during a Tkachenko oscillation. This profile offers some insight into why our experimental technique of altering the condensate profile at the center, couples so nicely to the Tkachenko modes. They also suggest an alternate scheme of exciting these modes by modulating the radial trap frequencies, at the Tkachenko frequency, in order to couple to this density distribution. While so far untested, this suggestion would provide a way to perform frequency resolved spectroscopy of Tkachenko oscillations, which may one day prove useful.

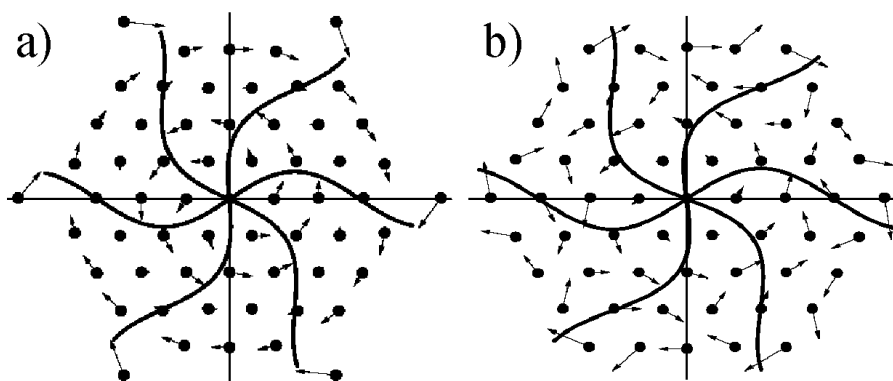


Figure 4.6: Figure taken from Ref. [83]. Plot a) and b) show the vortex lattice distortion resulting from a $(1,0)$ Tkachenko mode in the stiff and soft Thomas-Fermi regimes respectively. Dots show the equilibrium vortex positions and the arrows show the direction and magnitude of the calculated vortex displacements. In plot a) one can see the very ordered nature of the Tkachenko oscillation. A time evolution of this image shows that each vortex precesses along a highly elliptical path. In soft Thomas Fermi regime, plot b), individual vortex motion appears more chaotic as the lattice becomes compressible. A time evolution of this image shows that the precession of each vortex has become nearly circular. All vortices at the same radii precess in the same manner.